Effects of variable accelerations on a PHP-based cooling system

M Manzoni[1,5,*], M Mameli[1], C de Falco[2], L Araneo[3], S Filippeschi[4], M Marengo[1,5]

[1] *University of Bergamo, Department of Engineering and Applied Science, Italy*
[2] *Politecnico di Milano, MOX Mathematics Department, Italy*
[3] *Politecnico di Milano, Energy Department, Italy*
[4] *University of Pisa, DESTEC, Italy*
[5] *University of Brighton, School of Computing, Engineering and Mathematics, UK*

[*]*Corresponding author: miriam.manzoni@unibg.it*

ABSTRACT

A PHP is a passive, wickless heat transfer device consisting of a capillary loop, evacuated and partially filled with a working fluid, with alternated heating and cooling zones. The PHP light structure ($4kg/m^2$), flexibility and moderately high heat transfer capability ($30W/cm^2$) are interesting for automotive cooling applications. During their motion, vehicles withstand different speeding-up, which may influence the PHP behavior. The braking and the turning accelerations are the most critical reaching over $\pm1g$ for passenger cars, more for sport cars. Therefore, numerical simulations have been carried out to analyze the performances of a stand-alone PHP-based cooling system under transient accelerations.

KEYWORDS

Pulsating heat pipe, Two-phase flow, Acceleration effects, Cooling system

1   INTRODUCTION

In the past decades, the need of the automotive industry to become environmental friendly has intensified. The more and more stringent targets for CO_2 production, the request for particulate reduction and the lack of fossil resources led to the development of electric vehicles (e.g. Hybrid Electric Vehicles, Fuel Cell Electric Vehicles) able to combine different power sources. In addition, the great advance in electronics and micro-electronics induced even tradition cars to get "electronics addicted".

NOMENCLATURE

Latin symbols

A	Cross flow area, [m^2]	R_{eq}	Equivalent Thermal Resistance
A_{ex}	External lateral area, [m^2]	Re	Reynolds number, []
A_{w-f}	Internal lateral area, [m^2]	T	Temperature, [K]
a	Acceleration, [ms^{-2}]	t	Time, [s]
c_v	Specific heat constant volume, [Jkg^{-1}K^{-1}]	u	Velocity, [ms^{-1}]
f_τ	Friction coefficient, []	x	Axial coordinates, [m]
g	Gravity acceleration, [ms^{-2}]	**Greek symbols**	
h	Convection coefficient, [Wm^{-2}K^{-1}]	ρ	Density, [kg/m^3]
h_{LV}	Latent heat of vaporization, [Jkg^{-1}]	ε	Surface roughness, [m]
i	Vapor plugs index, []	ϑ	Inclination to horizontal, [rad]
j	Liquid slugs index, []	**Subscripts**	
k	Thermal conductivity, [Wm^{-1}K^{-1}]	$cond$	Condenser zone
K	Wall slices index, []	$heat$	Heater zone
L	Length, [m]	ex	External
m	Mass, [kg]	hom	Homogenous phase change
m_{LV}	Evaporated/Condensed mass, [kg]	het	Heterogeneous phase change
p	Pressure, [Pa]	int	Internal
Pr	Prandtl number, []	l	Liquid
$\dot{Q}$	Heat power, [W]	sat	Saturated conditions
q_{ex}	External heat flux, [Wm^{-2}]	v	Vapor
q_{w-f}	Heat flux between wall and fluid, [Wm^{-2}]	w	Wall
r	Tube internal radius, [m]	∞	Environmental

However, batteries and electronic components generate heat; optimum thermal performance and high reliability throughout the product life cycle are required key factors, even if the thermal environment of a motor compartment is extreme. In order to maximize the electronics performances and lifetimes, a precise temperature and temperature gradient control is requested.

Many different technologies are available for the thermal management of such systems: air cooling, forced liquid loops and phase change materials. In case of very high heat input fluxes, a possible solution lies in two-phase systems which make use of the high efficient thermal transport process of evaporation and condensation to maximize the thermal conductance and reduce the temperature gradient between a heat source and a heat sink. As relatively new and promising members of the wickless heat pipes family, Pulsating Heat Pipes (PHPs) have recently reached the attention of the automotive industry as a practical way to remove heat from the electronic components, [1], [2].

Patented by Akachi [3], [4] in the earlier '90es, a PHP consists of a capillary tube closed end to end in a loop, evacuated and partially filled with a working fluid. Since the tube diameter is small enough, the fluid usually distributes itself in a constraint pattern of vapor plugs and liquid slugs (Fig. 1). When power is provided at the heater section, evaporation occurs within the liquid phase, vapor pressure raises inducing oscillation and circulation of the fluid along the channel. Thus, the train of fluidic elements is

pushed toward the condenser zone where condensation occurs and both sensible and latent heat are rejected to an external cold source. Even if slug and plug is the most common hydraulic regime within a PHP, other possible fluidic paths characterized by separation of vapor and liquid can appear (e.g. annular, stratification) [5]. In addition, if too much power is provided at the evaporator section evaporating all the working fluid, the PHP reaches the unwanted condition of dry-out showing very poor thermal performances.
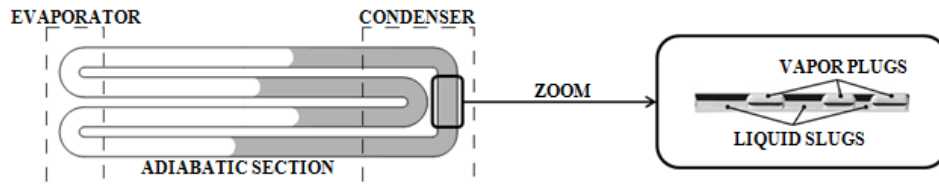
Figure 1 - Schematic of a generic PHP.

During their motion, vehicles withstand different accelerations, which must be accounted for in the design of their sub-systems. Speed and acceleration are very intrinsic to vehicle classes and traffic conditions. Usual accelerations for cars and heavy vehicles are fractions of g, but even more high values can be reached during particular sudden maneuvers (e.g. breaking and cornering): over ±1g for a passenger car and even more for sport cars.

The complex PHP thermal-hydraulic behaviour mainly depends on the interplay between phase change phenomena, capillary forces, and possible acting accelerations. The coupled effect of such phenomena, however, has not been thoroughly examined yet. The very few studies performed on planar PHPs operating under different acceleration loads [6], [7], [8], [9] have shown a strong relationship between PHP performances and applied accelerations. Most of these studies, however, are focused only on the steady-state conditions. Mameli et al. [9] presents also transient results underling a rapid response of the PHP thermal behavior to variation of the acceleration field for a very large range of g-levels. However, no tests have been performed at negative g-conditions (i.e. accelerations from the heater to the cooler zone). Thus, a validated numerical analysis appears as a useful tool in order to predict the transient response of a hypothetic PHP-based cooling system to sudden manoeuvres, which implies both positive and negative levels of acceleration.

Therefore, in the present work, numerical simulations have been carried out to analyze the performances of a PHP-based cooling system under variables accelerations from 2g to -2g (worst scenario). The employed one-dimensional lumped parameter numerical tool has been developed improving Mameli et al. [10], [11] previous code and consists of a two-phase separated flow model where capillary slug flow is assumed a priori. A complete set of balance differential equations accounts for thermal and fluid-dynamic phenomena. The originality of this numerical tool is the suppression of the standard assumption of saturated vapor plugs as well as the consequent embedding of heterogeneous and homogeneous phase changes. Moreover, vapor is not treated as an ideal gas anymore, but Van der Waals equation has been implemented. This tool has

already been validated against experimental data under different gravity steady conditions [12], [13].

2   NUMERICAL MODEL

The proposed model is applicable to PHPs in confined operating regimes (i.e. slug flow). Its main assumptions are:
a. The model is one-dimensional. Mass, momentum and heat transfer are calculated along the axial direction. Heat transfer in radial direction is lumped.
b. Liquid slug momentum equation is lumped. Friction between vapor and wall elements is neglected.
c. Liquid menisci maintain spherical shape with negligible contact angle at the wall.
d. Vapor may exist in saturated or not saturated conditions.
e. Vapor is treated as real gas. Density is calculated as mass over volume. Vapor pressure is defined as function of temperature and density (Van der Waals equation).
f. All other fluidic thermo-physical properties are standardly calculated as polynomial functions of temperature only. Liquid slugs pressure is set equal to the average value of the adjacent vapor plugs pressure.
g. The liquid film around each vapor plug is constant in space and time.

2.1 Fluidic model
Liquid slugs and vapor plugs are spatially traceable during the whole simulation time. A Lagrangian approach is applied in order to follow each fluidic element in its chaotic motion within the channel. In addition liquid slugs are subdivided into smaller domains characterized by the same velocity and pressure but, eventually, different temperatures. Fig. 2 shows a schematic of the numerical domains.
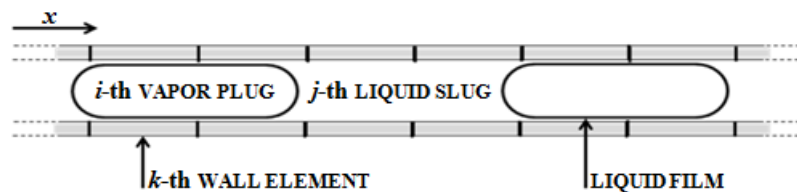

Figure 2 - Numerical domains. Liquid slugs sub-domains are not indicated.

2.1.1 Phase changes
Since the PHP tube is a closed domain, the total mass of fluid remains constant during the simulation time. However, the mass of single fluidic elements could vary due to phase changes. Heterogeneous and homogenous evaporation/condensation must be taken into account because of assumption *d*.
Heterogeneous condensation/evaporation can occur when a vapor/liquid comes into contact with a surface that has a temperature below/higher than the fluid one. This involves heat transfer to/from the solid wall.

Otherwise, if vapor/liquid pressure is higher/lower than the saturation value at its actual temperature, homogeneous condensation/evaporation occurs in the fluidic bulk. In order to evaluate the heat exchange between liquid slugs and vapor plugs due to this kind of transition the equivalent homogeneous heat is evaluated a posteriori as in Eq. 4.

Heterogeneous evaporated or condensed mass, $m_{LV,het}$, could be calculated as in Eq. 1. According to Fig. 3, a double check on pressure and temperature must be performed to assert if this kind of phase change may take place: if liquid pressure is lower than the saturation value or its temperature overcomes the saturation point, then evaporation occurs; if vapor pressure exceeds the saturation value or its temperature is lower than the saturation point, then condensation occurs. In both cases, the wall temperature T_w must satisfy a proper condition.

$$m_{LV,het} = \int_0^{\Delta t^*} \frac{A_{w-f} q_{w-f}}{|h_{LV}|} dt \quad if \begin{cases} evaporation: & T_w \geq T_l + \Delta T_{superheat} \\ condensation: & T_w \leq T_v - \Delta T_{supercool} \end{cases} \quad (1)$$

where $\Delta T_{superheat}$ and $\Delta T_{supercool}$ are fixed (see Table 2); A_{w-f} is the contact surface area between each solid domain and the fluidic elements, q_{w-f} is the heat exchanged between the wall and the fluidic elements (section 2.3), h_{LV} is the heat of vaporization and Δt^* is a characteristic time associated to new fluidic elements generation:

$$\Delta t^* = m_{min} \left(\frac{A_{w-f} q_{w-f}}{|h_{LV}|} \right)^{-1} \quad (2)$$

A new element is, indeed, produced only if $m_{LV,het} \geq m_{min}$, otherwise the mass exchange occurs only between adjacent elements; Δt^* is proportional to the evaporation/condensation ratio at steady state, while m_{min} is calculated assuming that every new element must have at least the volume of a sphere whose diameter is equal to the tube internal one $(m_{min,eva(cond)} = \frac{4}{3} \pi r^3 \rho_{v(l)})$. For the present operative conditions, the evaporative and condensed Δt^* are respectively 5×10^{-3} s and 1.5 s.

According to Fig. 3, if vapor pressure exceeds the saturation value at the actual temperature, homogeneous condensation occurs in the vapor bulk; if vapor pressure is lower than the saturation point, then homogeneous evaporation is induced in the adjacent liquid elements. Homogeneous evaporated or condensed mass, $m_{LV,hom}$, could be calculated at each time step by solving the simple linear systems of Eq. 3.

$$\begin{array}{ll} Evaporation \quad p < p_{sat} & Condensation \quad p > p_{sat} \\ \begin{cases} m_{LV,hom} = A\rho_{sat}L_{sat} - A\rho_v L_v \\ L_{sat} = L_v + \dfrac{m_{LV,hom}}{A\rho_l} \end{cases} & \begin{cases} m_{LV,hom} = A\rho_v L_v - A\rho_{sat}L_{sat} \\ L_{sat} = L_v - \dfrac{m_{LV,hom}}{A\rho_l} \end{cases} \end{array} \quad (3)$$

where *A* and *L* are the fluidic element cross section area and length, while *p* and *ρ* are its pressure and density. The sub-scripts *v* refers to vapor plugs, *l* to liquid slugs and *sat* to saturated conditions.

The heat released/requested during homogeneous phase changes at each time step Δt is calculated as:

$$Q_{hom} = \pm \frac{m_{LV,hom}|h_{LV}|}{\Delta t} \begin{cases} - & evaporation \\ + & condensation \end{cases} \tag{4}$$

For both kind of phase changes, if $m_{LV,het(hom)}$ exceeds the mass of the corresponding fluidic element, then this vanishes and the adjacent slugs/plugs merge.
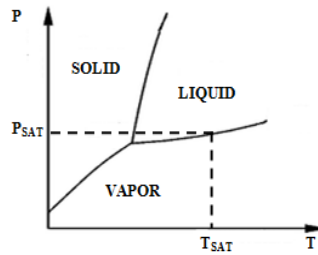

Figure 3 - Phase change diagram of a generic working fluid.

2.1.2 Momentum equation

The momentum equation is calculated for liquid slugs only. Vapor plugs are, therefore, drag along the tube by the liquid motion. Accounting for assumption *b*, the momentum equation of the *j*-th liquid slug integrated along its length is:

$$\frac{d(mu)}{dt} = mgsin(\vartheta) + A(p_i - p_{i+1}) - 0.5f_\tau \frac{m}{2r}u^2 \tag{5}$$

where *u* is the velocity and *r* the tube internal radius. The first term on the right side is the gravity force: ϑ is the local angle between the gravity vector and the flow direction. The second and the third terms are the forces due to adjacent vapor (i and $i + 1$) expansion/compression and to viscous losses. Pressure drop due to capillary forces has been neglected since the cross section along the tube length is constant and because of assumption *c*.

The friction coefficient f_τ is evaluated by means of semi-empirical correlations, either for fully developed laminar (i.e. Hagen-Poiseuille) [14] or turbulent flow (i.e Haaland) [15]. Minor losses are evaluated only if the j-th liquid slug passes through a bend. The friction coefficient is evaluated according to Darby 3K method [16], [17].

The solution of Eq. 5 provides the velocity of each liquid slug. Their new position for each time step $x_{j,t}$ can be estimated as in Eq. 6 where a is the *j*-th liquid slug acceleration defined as the ratio between the forces applied on the fluidic element and its mass.

$$x_t = x_{t-1} + u\Delta t + 0.5a\Delta t^2 \tag{6}$$

If the spacing between two adjacent fluidic elements is zero or if there is an overlap, they merge and the total number is accordingly reduced.

2.1.3 Energy balance
Fluidic temperatures are calculated by solving the energy balance applied to each lagrangian sub-domain.

$$c_v \frac{d(Tm)}{dt} = \left(q_{w-f}A_{w-f} - m_{LV.het}h_{LV}\right) - \left(kA\frac{\partial T}{\partial x}\Big|_i^j + kA\frac{\partial T}{\partial x}\Big|_{i+1}^j\right) - p\frac{dV}{dt} + Q_{hom} \tag{7}$$

where c_v and k are the specific heat and the thermal conductivity. These equations apply for each of the phases. The first term on the right side of Eq. 7 represents the heat exchanged between the wall and the fluidic elements, the second is the axial conduction within the fluid, the third term is the compression work calculated only for vapor plugs and the last term is the heat associated to homogenous phase changes.

2.2 Solid model
The PHP tube is sub-divided into smaller Eulerian domains with constant mass and fixed position over time. Therefore, only the energy equation must be implemented in order to evaluate the PHP wall temperature.

$$m_w c_{v,w} \frac{dT_w}{dt} = q_{ex}A_{ex} - k_w A_w \left(\frac{\partial T_w}{\partial x}\Big|_{K-1}^K + \frac{\partial T_w}{\partial x}\Big|_{K+1}^K\right) - q_{w-f}A_{w-f} \tag{8}$$

where A_{ex} is the contact area between the wall and the external environment and A_w the tube wall cross section area.

The second term on the right side of Eq. 8 accounts for the heat conduced within the wall, the third term is the heat exchanged between the wall and the fluidic elements (section 2.3), while the first term is the heat exchanged between the wall and the external environment.

Constant heat input power Q_{ex} is supplied to the evaporator zone; forced convection is applied at the condenser; no heat exchange occurs between the wall and the environment in the adiabatic region.

$$q_{ex} = \begin{cases} Q_{ex}/A_{ex} & evaporator \\ 0 & adiabatic\ zone \\ h_\infty(T_w - T_\infty) & condenser \end{cases} \tag{9}$$

where h_∞ is a constant external heat transfer coefficient (Tab. 1). External air is assumed at constant temperature T_∞. The radiative heat loss has been neglected since it has been estimated as ~0.1% of q_{ex}.

2.3 Solid/fluid coupling

Solid and fluidic domains are routinely coupled by the heat exchange between wall and slugs (plugs):

$$q_{w-f} = h(T_w - T) \tag{10}$$

where *h* is the chosen heat transfer coefficient.

If no phase changes occur, *h* can be estimated by means of different semi-empirical formula: Shah and London correlation [18] is used for the laminar flow thermally developing region ($Re \leq 2000$), the Gnielinski correlation [14] is implemented for the transient/turbulent flow ($2000 < Re < 10000$), while for the fully developed turbulent flow ($Re \geq 10000$) Dittus-Boelter correlation [14] is applied.

If phase changes occur, constant heat transfer coefficients have been presently assumed: 2000 W/m^{2}K for condensation and 4000 W/m^{2}K for evaporation. The values are chosen accounting for the coefficients usually identified in literature [5].

3   NUMERICAL RESULTS

The numerical simulations have been performed for an ideal planar PHP, meaning that the thermal inertia of the peripheral elements has been neglected. The physical and numerical characteristics of the tested design are listed in Tab. 1 and Fig. 4. The device dimensions and the heat input fluxes have been chosen in feasible ranges for electronics cooling. The provided power is kept constant during the whole simulation time to test the device in the worst load condition. The temperature of the external environment has been set thinking of a PHP cooled down by forced convection from a radiator in contact to the ambient outside the car motor hood.

Since fixed flux at the evaporator (Q_{ex}) and fixed temperature at the condenser (T_{∞}) have been imposed as boundaries conditions, the heat rejection rate is an output of the model and it equals the heat input rate when stationary conditions are reached.
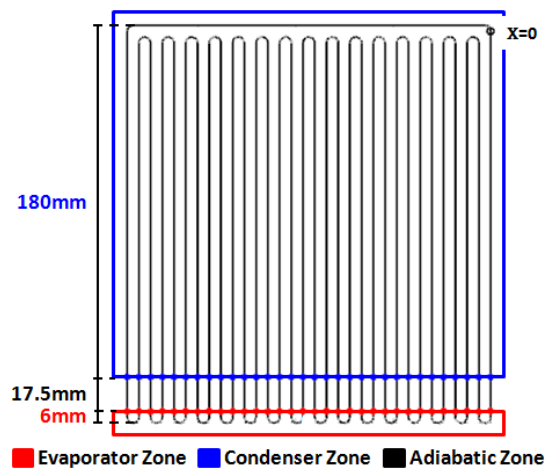

Figure 4 - PHP dimensions.

Input parameter	Value	Input parameter	Value
Working fluid	FC-72	Lateral acceleration	-2g / 2g
Volumetric filling ratio	0.5	External temperature	20 °C
Tube material	Copper	External HTC	300 W/m^{2}K
Internal diameter	1.1 mm	Evaporator heat flux	3.23 W/cm^2
External diameter	2.0 mm	ΔT superheat	2.5 °C
Surface roughness	50 μm	ΔT cooling	0.1 °C
Total length	6.62 m	N° of wall grids	430
N° of *U* bends	31	N° of slug/plug (t=0)	20
Gravity acceleration	1g	Time step	0.001 sec

Table 1 - PHP physical and numerical characteristics.

The results are presented in form of temperature responses to accelerations and decelerations since temperature control is the key parameter for electronic cooling once the heat input is known.

The model is one-dimensional, thus only accelerations parallel to the fluidic path can be accounted for. Since the cornering and the breaking acceleration of a car lay in the plane perpendicular to the gravity direction, in order to study their effect on the PHP performance, a horizontal orientation has first been tested (Fig. 5). The employed coordinate system is also displayed in Fig. 5.
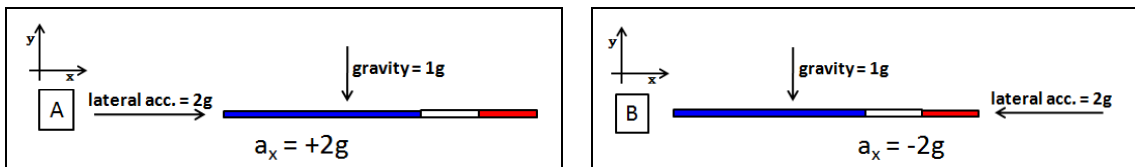

Figure 5 - Schematic of the horizontal simulated cases. Condenser zone in blue, evaporator zone in red.

The simulations have been carried out providing a step variation (10s) of the acceleration acting on the system, which previously has reached steady state. This tries to reproduce sudden breaking or cornering maneuver ($\pm 2g$) of a car in uniform motion (e.g. a car on a highway). The results in term of PHP averaged wall temperature are presented in Fig. 6.

The ideal capillary PHP shows a quick response to sudden modifications of the acceleration acting along the fluid path direction improving its performances, because the new associated force increases the fluid circulation helping the liquid to reflow from the condenser to the evaporator zone (Case A). When the disturbance disappears, the PHP returns to its normal steady state. A negative acceleration, otherwise, does not provide any variation on the PHP performances (Case B).

The absence of acceleration, as well as the application of an acceleration directed from the evaporator to the condenser zone, indeed, damps the fluid motion and thus the phase

changes within the system. The device works like a tube full of liquid and vapor, which transports heat only by axial conduction with, consequently, higher temperatures.
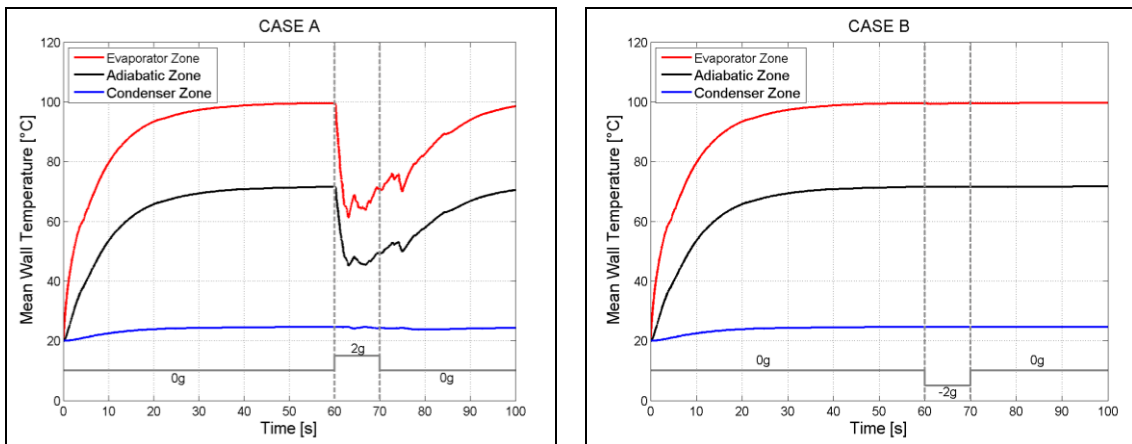

Figure 6 - Horizontal PHP thermal response to acceleration step variation in the PHP plane. Normal gravity constant.

This explanation is also supported by Fig. 7, which shows a particular of the liquid velocity during the acceleration step. It is clearly visible that the velocity assumes not zero values only when +2g is applied on the system; the application of -2g induces a first oscillation on the velocity signal that, however, is quickly recovered.
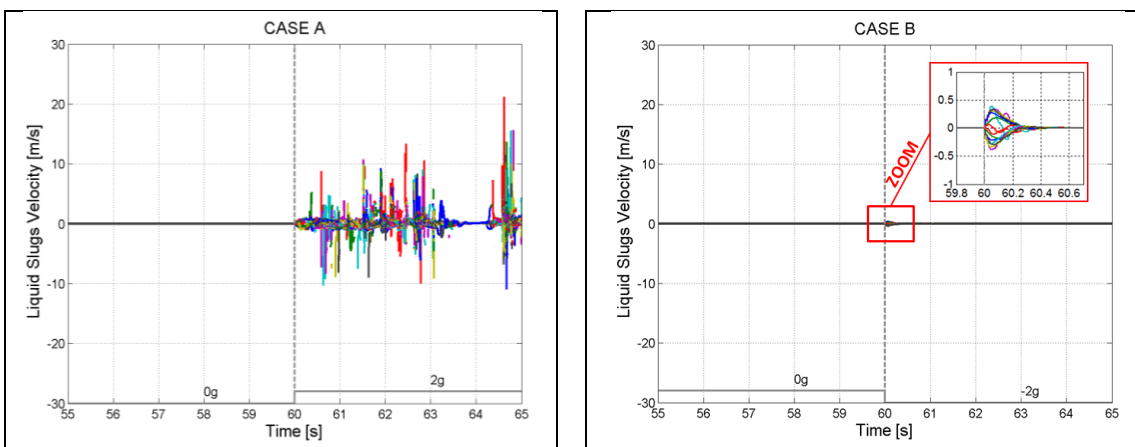

Figure 7 - Particular of the liquid velocity during the acceleration step. Each color is associated to its own slug.

3.2 Inclined PHP

Since the PHP performances are better when a force is applied continuously from the condenser to the evaporator zone, simulations have been carried out for a 45° inclined PHP (Fig. 8) in order to reduce the PHP thermal resistance during vehicles uniform motion.
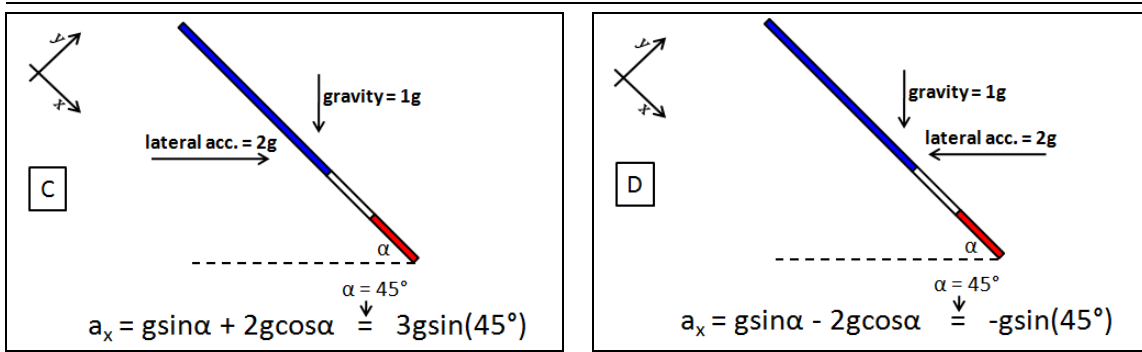
Figure 8 - Schematic of the 45° inclined simulated cases. Condenser zone in blue, evaporator zone in red.

The results in term of PHP mean wall temperature are presented in Fig. 9. Again, like in the case of the horizontal PHP, the system shows a quick response to acceleration step improving its performances when the acceleration is increased (Case C), worsening them otherwise (Case D). This last simulation also shows that the recovery after the acceleration step is very rapid, meaning that the PHP is a robust system with respect to variation of the acceleration level. Moreover, it should be notice that, since the simulated PHP is stand-alone, its transient response is quicker with respect to a real device due to peripheral elements thermal inertia. This implies that the temperature enhancement shown for the Case D is hereby amplified (conservative situation).
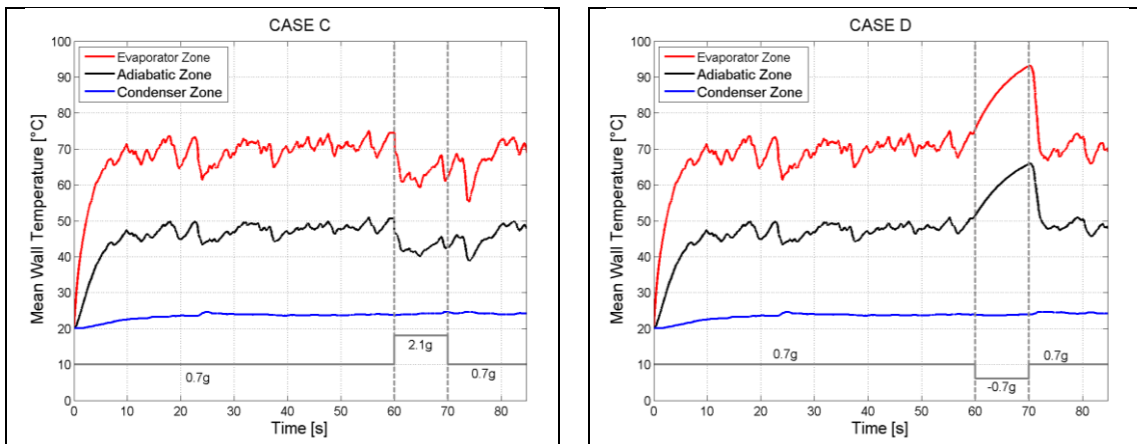

Figure 9 - Inclined PHP thermal response to acceleration step variation.

Case C underlines, also, that the PHP temperature characteristics are not so different for such positive variations of the acceleration level. This can also be deduced from Fig. 10, which shows the equivalent thermal resistance of the device, as:

$$R_{eq} = \frac{T_{ev} - T_{cond}}{\dot{Q}} \tag{11}$$

where the numerator represents the difference between the evaporator and the condenser average temperatures in the pseudo-steady state, while $\dot{Q}$ is the external heat power.

The calculation of the PHP equivalent thermal resistance displays great improvements of the PHP performances only when passing from negative/zero to positive accelerations. This is an interesting aspect meaning that if the device is designed/oriented such as it senses only positive accelerations for all the vehicle maneuvers, the performances of the PHP remain quite constant over time.
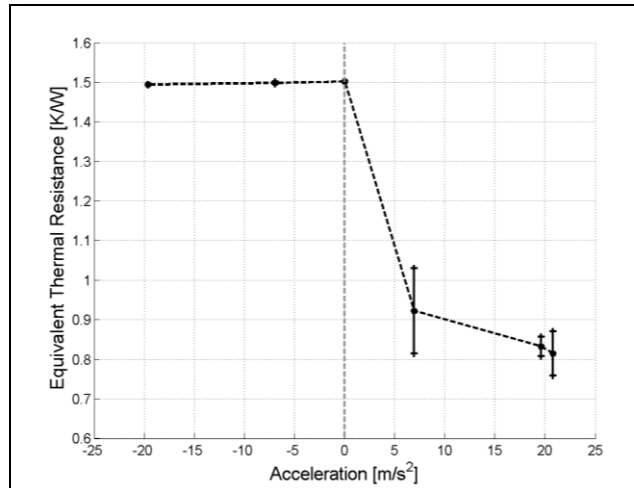

Figure 10 - PHP equivalent thermal resistance for different accelerations.

4   CONCLUSIONS

The thermal performances of an ideal PHP-based cooling system have been simulated for transient step variation (10s) of the applied acceleration from 2g to -2g. An already validated one-dimensional lumped parameter numerical tool has been employed for such analyses. Since the model is one-dimensional, only accelerations parallel to the fluidic path can be accounted for. Thus two different orientations ($\alpha = 0°, \alpha = 45°$) have been considered in order to study the combined effect of gravity and sudden cornering/breaking accelerations. The results can be summarized in the following points:

− If no acceleration is applied on the system, the PHP behaves like a tube full of liquid and vapor that transmits heat only by conduction with associated relative high temperatures.

− The PHP shows a quick response to positive accelerations improving its performances since the associated force helps the liquid to flow from the condenser to the evaporator zone.

− Negative accelerations damp the fluid motion worsening the PHP performances. The recovery from negative to positive accelerations is very rapid, meaning that the system is robust to variation of the acceleration levels.

− The equivalent thermal resistance is not so influenced by variation of positive accelerations, meaning that if the PHP-based cooling system is designed/oriented

such as it senses only positive accelerations during all the vehicle maneuvers, its performances remain quite constant over time.

Thus, a PHP represents an innovative, valid candidate for automotive electronics cooling, not only for its light structure, flexibility and reasonable heat transfer capability, but also for its robust behavior with respect to variation of the acceleration levels.

REFERENCE LIST

[1] Poláŝek, F., & Štule, P. (1997). Thermal control of IGBT modules in traction drives by pulsating heat pipes. *Proc. of 10th International Heat Pipe Conference*.

[2] Akachi, H. & Miyazaki, Y. (1997). Stereo-type heat lane heat sink. *Preprints 10th Internat. Heat Pipe Conf.*

[3] Akachi, H. (1990). *US Patent* No. 4921041.

[4] Akachi, H. (1993). *US Patent* No. 5219020.

[5] Mameli, M., Marengo, M., & Khandekar, S. (2014). Local heat transfer measurement and thermo-fluid characterization of a pulsating heat pipe. *Int. J. of Thermal Sciences*, **45**, 140-152.

[6] Kiseev, V.M., & Zolkin, K.A. (1999). The Influence of Acceleration on the Performance of Oscillating Heat Pipe. *Proc. of the 11th International Heat Pipe Conference.*

[7] Van Es, J., & Woering, A.A. (2000). High-acceleration performance of the Flat Swinging Heat Pipe. *NLR-TP-2000-265*.

[8] Gu, J., Kawaji, M., & Futamaca, R. (2004). Effect of gravity on the performance on pulsating heating pipe. *J. of Thermophysics and Heat Transfer*, **18**, 370-378.

[9] Mameli, M., Manzoni, M., Araneo, L., Filippeschi, S., & Marengo, M. (2014). Experimental investigation on a closed loop pulsating heat pipe in hyper-gravity conditions. *Proc. of the 15th IHTC Conference.*

[10] Mameli, M., Marengo, M., & Zinna, S. (2012). Thermal simulation of a pulsating heat pipe: effects of different liquid properties on a simple geometry. *Heat Transfer Engineering*, **33**, 1177-1187.

[11] Mameli, M., Marengo, M., & Zinna S. (2012). Numerical model of a multi-turn closed loop pulsating heat pipe: effect of the local pressure losses due to meanderings. *Int. J. Heat Mass Transfer*, **55**, 1036-1047.

[12] Manzoni, M., Mameli, M., DeFalco, C., Araneo, L., Filippeschi, S., & Marengo, M. (2014). Towards a numerical simulation of a closed loop pulsating heat pipe in different gravity levels. *Proc. of the 32nd UIT Conference.*

[13] Manzoni, M., Mameli, M., DeFalco, C., Araneo, L., Filippeschi, S., & Marengo, M. (2014). Toward a design of a micro pulsating heat pipe. *Proc. of 4th European Conference on Microfluidics.*

[14] Incropera, F. P., & DeWitt, D. P. (2007). Chapter 8: Internal Flow. *Fundamentals of Heat and Mass Transfer*, 6th Ed.

[15] Haaland, S. (1983). Simple and Explicit Formulas for the Friction Factor in Turbulent flow. *Transactions of ASME, Journal of Fluids Engineering*, **103**, 89-90. Darby, R. (1999). Correlate pressure drop through fittings. *Chemical Engineering*,**106**,101-104.

[16] Darby, R. (2001). Correlate pressure drop through fittings. *Chemical Engineering*, **104**,127-130.

[17] Shah, R. K., & London, A. L. (1978). Laminar Flow Forced Convection in Ducts. *Advanced in Heat Transfer*, Supple. 1.